Journal of Casting & Materials Engineering Vol. 4 No. 4 (2020) 58–64
https://doi.org/10.7494/jcme.2020.4.4.58

An Evaluation of the Effect of Ultrasonic Degassing on Components Produced by High Pressure Die Casting

Manel da Silva[a]*, Attila Bajusz[b], Thomas Pabel[c], Tose Petkov[c], Xavier Plantà[d]

[a]Eurecat, Centre Tecnològic de Catalunya, Unitat de Materials Metàl•lics i Ceràmics. Avda. Universitat Autonoma 23, Cerdanyola del Vallès, 08290, Spain
[b]Certa Kft., Sátoraljaújhely, 3980, Hungary
[c]Austrian Foundry Research Institute, 8700 Leoben, Austria
[d]Ultrasion, S.L., Cerdanyola del Vallès, 08290, Spain
e-mail: manel.dasilva@eurecat.org

© 2020 Authors. This is an open access publication, which can be used, distributed and reproduced in any medium according to the Creative Commons CC-BY 4.0 License requiring that the original work has been properly cited.

Received: 1 November 2020/Accepted: 23 December 2020/ Published online: 18 January 2021
This article is published with open access at AGH University of Science and Technology Press

Abstract

Ultrasonic treatment is known to be efficient for aluminium melt degassing with the additional benefits of being both economical and environment friendly. This paper describes the effect of ultrasonic degassing on the preparation of an AlSi9Cu3(Fe) alloy for High Pressure Die Casting (HPDC). The degassing efficiency was assessed in terms of the indirect evaluation of the melt, by means of the reduced pressure test and the porosity evaluation of the cast parts. Additionally, the corresponding hydrogen content was estimated with an experimental equation reported in the literature. Ultrasonic degassing shows greater efficiency in terms of hydrogen removal from the melt than conventional N_2 + Ar lance bubbling. Components produced by HPDC without degassing, with ultrasonic degassing and with lance degassing, were analysed by computed tomography and by metallography. The results show that the components produced by HPDC after ultrasonic degassing have a similar porosity level to components degassed with conventional lance bubbling, both showing an important improvement over components produced without degassing treatment. Hardness values were similar for all different treatment conditions and well over the minimum value established for the alloy by the corresponding standard.

Keywords:
aluminium alloy, casting, HPDC, degassing, ultrasonic treatment, hydrogen

1. INTRODUCTION

Hydrogen solubility is relatively high in liquid aluminium and very low in solid aluminium. As a result, the excess hydrogen precipitates during solidification and in most cases gets trapped between solid aluminium grains, forming gas porosity or adding to shrinkage porosity. Porosity is one of the main defects encountered in casting parts and causes poor ductility, low fatigue resistance and reduced strength of the casting. Degassing has become a crucial operation in high quality casting [1].

The dissolved hydrogen present in liquid aluminium mainly comes from atmospheric moisture as water vapour reacts with aluminium to produce alumina and hydrogen. Hydrogen solubility in aluminium is directly correlated to alloy temperature and humidity ratio, therefore lowering the temperature can cause the aluminium to be supersaturated by hydrogen that will tend to naturally degas to the so-called quasi-equilibrium hydrogen level [1–3]. Ultrasonic degassing has the advantage of being able to reach a hydrogen level 50% lower than the quasi-equilibrium concentration [2]. This level of degassing is inevitably followed by natural re-gassing to the quasi-equilibrium level, but this low level of hydrogen can be retained if casting happens shortly after degassing is finished [3].

Ultrasonic degassing of liquid metals has a long history. As early as the 1940s, Esmarch et al. studied the degassing of Al-Mg alloys by vibrations in a crucible and sonic vibrations induced by contactless electromagnetic stirring and [4]. In 1950 Bradfield reported the works of Turner on the degassing of molten aluminium and its alloys by means of the direct introduction of ultrasonic oscillations into the melt at 15 kHz and 26 kHz [5]. Starting from the 1960s, successful laboratory and pilot-scale trials of ultrasonic degassing for foundry and later wrought alloys were performed and summarized in a series of publications by G. Eskin [2, 6]. In these works, the solution to practical issues such as equipment (water-cooled magnetostrictive transducers)

and sonotrode materials selection (Nb and Nb-based alloys) were presented and justified; and several practical recommendations were made regarding the degassing schemes and the number of sonotrodes per treated volume [6].

The efficiency of ultrasonic degassing is a function of input ultrasonic power, melt flow, melt temperature, and alloy composition. The fundamental studies on these issues have been published elsewhere [2, 3, 6].

Despite successful industrial trials in the 1960s and 1970s, ultrasonic degassing was not adopted as a mainstream technology due to the arrival of gas-assisted degassing, which steadily replaced little flux degassing treatment, a toxic degassing treatment. In recent years, the intrinsic features of ultrasonic degassing – such as no requirement for gas usage, no toxic or pollutants emissions – led to a reconsideration of this technology since it may answer the current environmental challenges. In addition, the new level of ultrasonic technology has made its application easier.

For this reason, in recent years researchers have been studying the effect that ultrasonic treatment has on metals. However, all these publications are related to laboratory trials, working with a few kilograms of metal [7–9] and very little work has been published regarding results obtained in large melt volumes at industrial scale.

The present paper reports the results of pilot-scale trials of ultrasonic degassing conducted in large volumes (500 kg of aluminium alloy) and the technology's effects on the final cast components produced by High Pressure Die Casting (HPDC), carried out in actual industrial facilities.

2. EXPERIMENTAL PROCEDURE

2.1. Ultrasonic degassing equipment

The experiments were conducted using a prototype specifically designed to treat large volumes of molten aluminium (Fig. 1). The device functioning is described in detail in a previous work, where the results were obtained for a much smaller volume (150 kg) of AlSi7Mg alloy and were compared with rotary degassing [10].

Fig. 1. Image of ultrasonic degassing prototype

The ultrasonic equipment used in the experiments was composed of a 5-kW USGC-5-22 MS ultrasonic generator, a 5-kW MST-5-18 water-cooled magnetostrictive transducer, a titanium booster, all supplied by Reltec (Russia), and a niobium multi-stage sonicator (Fig. 2). Figure 3 shows the assembled ultrasonic degassing equipment used in the experiments.

Fig. 2. Photograph of the stepped sonotrode used in the ultrasonic degassing tests

Fig. 3. Image of ultrasonic equipment used in the trials

2.2. Melt treatment procedure

AlSi9Cu3(Fe) (EN AC-46000) alloy was used for the trials. The treatment was conducted in a holding furnace with a capability of 500 kg, filled up to almost its maximum capacity (over 95%), as is shown in Figure 1. The alloy was previously molten in a tilting tower furnace and was transferred to the holding furnace with a standard transport ladle with a capacity of 200 kg, without performing any treatment or skimming process to the melt. The degassing treatment was conducted at a metal temperature of 690 ±10°C.

A stepped sonotrode as shown in Figure 2 was used to treat the molten metal during 15 min. During the ultrasonic treatment (US) the sonotrode was moved with the rotary crown of the prototype inducing circular movements at approximately 2/3 of the crucible diameter at a rotational speed of about 1 rpm [10]. Research conducted previously suggests that in order to treat large volumes the ultrasonic treatment must necessarily be long with a moving ultrasonic stream within the melt surface [3]. Ultrasounds with power between 4.0 and 4.5 kW in the range of 17–18 kHz were applied to the molten metal with an approximated vibration amplitude of 25 μm. Alternatively, a 15 min degassing treatment with a porous graphite lance bubbling an N_2 + Ar mixture, was introduced to the same amount of metal, with the same temperature and composition.

Indirect measurements of the hydrogen content with Reduced Pressure Test (RPT) (MK, Germany) were performed before and after the degassing treatment in the holding furnace. The values of the resulting Density Index (DI) were calculated form the extracted samples. The corresponding hydrogen content was calculated by applying an empirical equation reported in the literature for AlSi9Cu3(Fe) alloy [3].

2.3. Component casting and evaluation

The cast components were produced using a HPDC Unit (Weingarten 250 Tn) with a 50 mm plunger diameter, 3 m/s of injection speed and 180–220 bar of compacting pressure. For the casting production, the melt was transferred from the holding furnace to the shot sleeve with a rotary transport ladle. A standard production die of an actual industrial component was used to cast the specimens. Die lubrication and extraction of the part were done manually by an operator.

The HPDC components were produced in two different batches. From the 1st batch components were produced in three different ways; without treatment (W), with US treatment (0 holding time) and US1.5 (1.5 hours holding time after US treatment). From the 2nd batch, components were produced with a 15 min lance degassing treatment. The L (0 holding time) and L1 (after 1 hour holding time) components belong to this 2nd batch. One piece produced in each of these degassing conditions were analysed (treatment + waiting time).

The porosity of the selected parts (Fig. 4a), was analysed by computed tomography v|tome|x (with area detector DXR-250RT, magnification of 6.23, acceleration voltage of 180 kV, current of 200 μa, filter of 2 mm Al, exposure time of 333 ms and voxel size of 342.885 × 10^{-6} mm^3). This setup allows to detect pores with a minimum size of 140 μm.

The same parts were subsequently sectioned in order to measure their chemical composition, microstructure and hardness. Figure 4b shows the regions where the different specimens were extracted from. The chemical composition of these sections were analysed by optical emission spectrometry with a Spectrolab analyser from Spectro. An Olympus optical microscope was used for the microstructural analysis. The porosity of the polished specimens was quantified with Analysis software, at a magnification of 100×, what implies the screening of a total area of 1.63 mm^2 per image. A Zeiss Gimini Field Emission Scanning Electron Microscope (FE-SEM) was used to determine the different intermetallic phases present in the alloys with the aid of the Energy Dispersive Spectroscopy (EDS) detector.

The hardness of the components was determined with a Brinell HB10 (62.5 Kpf/2.5). A total of 6 indentations were performed in each component.

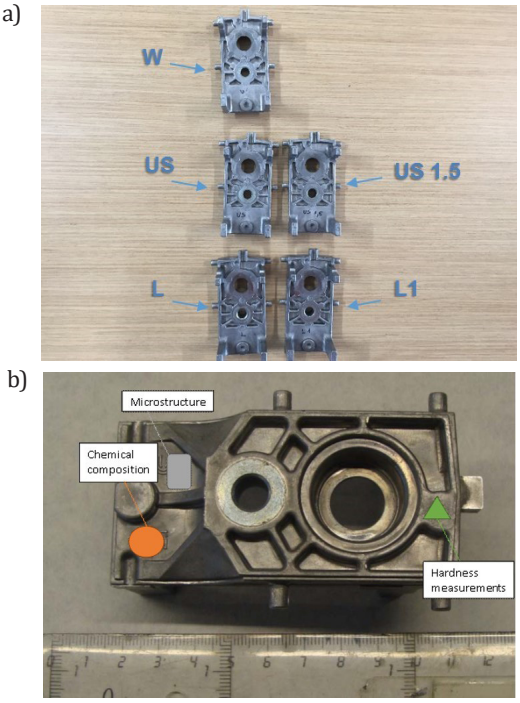

Fig. 4. Images of: a) the components selected for characterization; b) the location where the different characterization techniques were applied

3. RESULTS AND DISCUSSION

3.1. Melt quality

The results of the RPT measures conducted in the molten aluminium before and after the degassing treatments are presented in Figure 5. The graph shows the decrement of the DI after the corresponding degassing treatment. The DI values are much smaller after the US treatment, which shows that this treatment is much more effective than the lance degassing using an N_2+ Ar mixture.

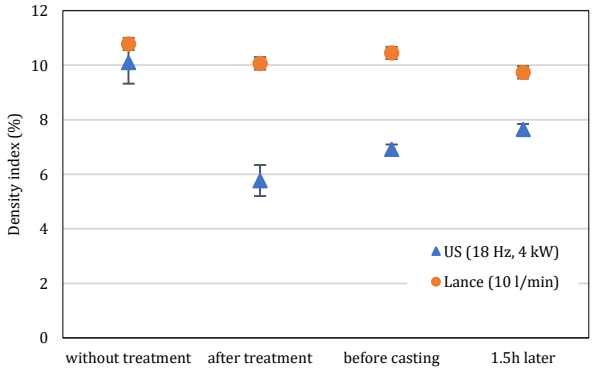

Fig. 5. Density index values obtained after ultrasonic treatment (US) and after lance degassing treatment (Lance)

The hydrogen content present in the melt can be estimated from Equation (1) [3]:

$$[H] = (DI + 0.0204)/0.5066 \quad (1)$$

The measured DI values and the corresponding hydrogen contents calculated with Equation (1) are presented in Table 1.

Table 1
Density Index values obtained in the melt analysis and their corresponding estimated hydrogen concentration

Treatment type	Ultrasounds		Lance bubbling	
Stage	DI (%)	H (cm^3/100 g)	DI (%)	H (cm^3/100 g)
Before treat	10.10	0.240	10.78	0.253
15 min after	5.77	0.154	10.07	0.239
Before cast	6.92	0.177	10.45	0.247
1.5 h later	7.65	0.191	9.74	0.232

These measurements show that, while ultrasonic degassing reduces the original DI values from about 11 to 6, the lance decreases the DI only to about 10, in the AlSi9Cu3(Fe) alloy. On one hand, these high DI values obtained for the lance degassing suggest that the degassing efficiency of this treatment is not as high as modern rotary degassing [11]. On the other hand, these values confirm that ultrasound is a more effective degassing method to remove H2 than the standard lance degassing treatment currently used by the foundry for the AlSi9Cu3(Fe) alloy. 36% lower hydrogen level was observed 15 minutes after the US degassing treatment than for lance degassing and this reduction remained still at 28% just before casting started

The values of DI and their corresponding equivalent hydrogen level slightly increases with the subsequent holding time in the case of the ultrasonic treatment. This effect can be attributed to the natural re-gassing taking place in the alloy, as it was already reported for AlSi9Cu3(Fe) alloy for smaller melt volumes. This phenomenon takes place after effective degassing treatment, i.e. those which reduce the hydrogen concentration below the corresponding quasi-equilibrium level of the melt [3].

On the other hand, the efficiency of lance degassing in such a large volume is quite small. The initial degassing effect is very small, decreasing the DI value from 11 to 10, and with the holding time, the DI values remain at the same level or even slightly decrease, suggesting that a natural degassing may still been taking place. The results suggest that lance bubbling in such large volumes is not an efficient means for aluminium degassing.

3.2. X-ray tomography analysis

The 3D reconstruction of the pore distribution obtained by the X-ray tomography is presented in Figure 6 for two of the die-casted components analysed, without treatment (W) (Fig. 6a) and treated with US (US) (Fig. 6b). The defects are concentrated in both cases in the lower part of the component, mainly in the junction between the main body and the two lower arms, as it can be observed in the images.

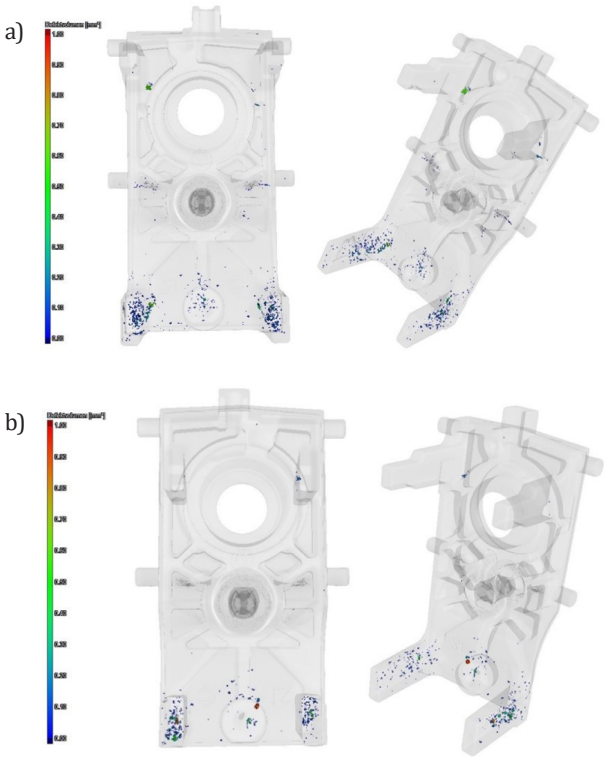

Fig. 6. 3D reconstruction of the porosity from the tomography images of: a) a part without degassing treatment; b) a part with ultrasonic degassing treatment

A comparison of the pores observed in the inspected components by X-ray tomography is presented in the form of a histogram in Figure 7. It can be observed that both degassing treatments considerably reduce the number of pores, especially of small pores, even though no difference can be observed in the porosity distribution of the parts produced by HPDC regarding the degassing treatment conducted, presumably due to the high porosity intrinsically related to this casting process [12].

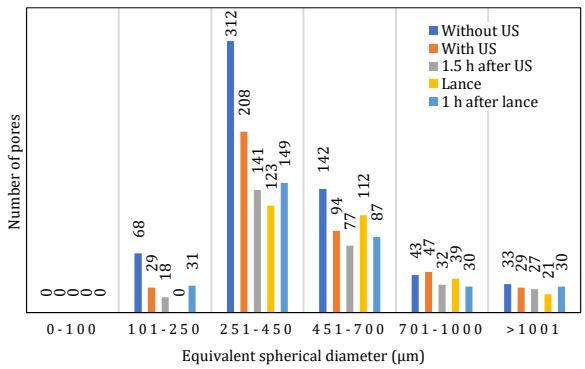

Fig. 7. Pore distribution for the different components measured by computed tomography

Therefore, the difference in degassing efficiency perceived from the DI values measured in the melt after the degassing treatment is diluted once the HPDC process is applied, obtaining components with a similar degree of porosity level.

3.3. Chemical composition and microstructure

The chemical composition of the two batches used to produce the components is presented in Table 2. The composition values of the batches are very similar and is in the composition range defined in the UNE-EN 1706-2011 standard for alloy EN AC-AlSi9Cu3(Fe).

Table 2
Chemical composition of the material used to produce the HPDC components

Batch	%Si	%Fe	%Cu	%Mn	%Mg	%Zn	%Pb
W-US	8.75	0.75	2.46	0.21	0.32	1.02	0.08
L	8.89	0.76	2.53	0.21	0.32	1.03	0.08
EN AC-AlSi9Cu3(Fe) UNE-EN 1706-2011	8–11	< 1.3	2–4	< 0.55	0.05 –0.55	< 1.2	< 0.35

The microstructure of the cross sections of the castings produced after any of the degassing treatments is typical for this type of alloy and consists of a primary Al-solid solution and (Al + Si)-eutectic. Figure 8 shows the microstructure of samples produced without treatment (W), with lance bubbling (L and L1) and with ultrasonic degassing (US and US1.5). Table 3 shows the results obtained from the porosity quantification performed on the polished specimens. It can be observed that the porosity level of the 5 specimens fell in the same range (between 0.1 and 0.6%), corroborating the results obtained by X-ray tomography, that porosities in both set of components are in the same level.

In addition to the main structural phases, isolated Fe-containing particles in the form of polygonal particles and of a needle shape were observed in the FE-SEM analysis (Fig. 9). These intermetallic phases are formed due to the presence of Fe in the alloy and, by contrast, these can be distinguished from Si particles. From the EDS analysis performed in the FE-SEM and from the phases reported in the literature for Al–Si–Cu alloys with similar composition [13], it is deduced that the Fe-containing intermetallic compounds present in the alloy are (Fe,Mn)3Si2Al15, polygonal phases (Spectrum 1), and FeSiAl5, elongated phases (Spectrum 4). It can be observed that Spectrum 4 has a high amount of Cu as well. As the elongated FeSiAl5 phases are quite narrow and are commonly surrounded by rich Cu phases, such as CuAl2, the area covered by the X-ray analysis contains also part of this surrounding material. In the microstructure there is no indication of over-modifications such as polygonal Al2Si2Sr intermetallic phases or coarsened Si-eutectic. Non-metallic inclusions, i.e. oxides and oxide films, were detected.

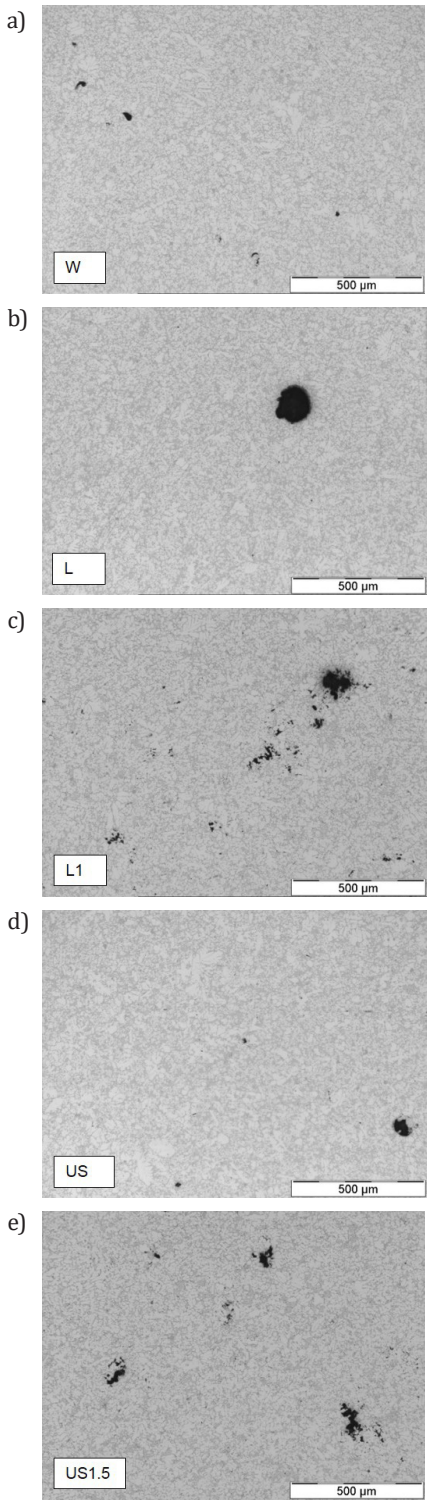

Fig. 8. Microstructure of the components: a) produced without heat treatment (W), b) produced immediately after applying the lance degassing treatment (L), c) produced after approximately 1 hour of production time (L1), d) produced after ultrasonic degassing treatment (US) and e) produced about 1.5 hours after the treatment (US1.5)

Table 3
Porosity values in the different HPDC components measured by quantitative metallography

Component ref.	W	L	L1	US	US1.5
Porosity (%)	0.13	0.1	0.58	0.23	0.28

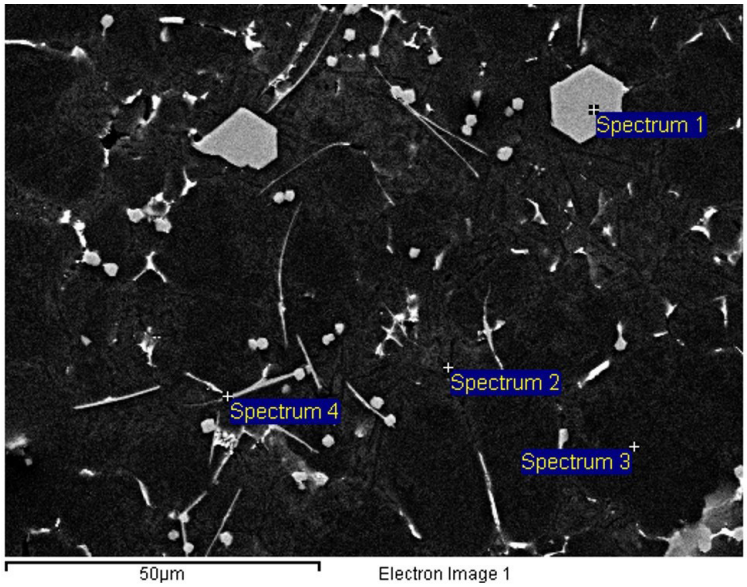

Processing option : All elements analysed (Normalised)

Spectrum	Al	Si	Cr	Mn	Fe	Ni	Cu	Zn	Total
Spectrum 1	59.12	9.59	1.68	7.91	19.70		2.00		100.00
Spectrum 2	83.77	12.56					2.28	1.39	100.00
Spectrum 3	98.21						0.89	0.90	100.00
Spectrum 4	65.33	10.19		0.78	6.16	0.64	15.07	1.83	100.00

Fig. 9. FE-SEM image with EDS analysis of the different phases observed in the AlSi9Cu3 alloy

3.4. Mechanical properties

The obtained values from the hardness measurements are shown in Table 4. The average hardness values of all the castings are in the range of 93–95 HB, which is well above the minimum hardness of 80 HB 5/250 required by UNE--EN 1706:2011 for AlSi9Cu3(Fe) alloy. No significant difference in hardness can be observed between the components produced with different degassing treatments.

Grain refining effect is commonly associated with ultrasonic treatment [14, 15], however, no evidence of it was observed with this experimental set-up. Even, if it is quite controversial to directly apply the Hall–Petch equation in Al-Si casting alloys, various authors have reported a clear relation between grain size, yield and tensile strength and hardness. Values of hardness and material strength increase with grain refinement [16–18].

Table 4
Brinell HB10 hardness obtained for the HPDC parts

Indentation	W	L	L1	US	US1.5
1	93	97	98	89	89
2	91	89	90	86	87
3	97	101	97	97	97
4	90	94	91	94	93
5	94	90	101	97	92
6	96	99	95	95	97
Average	94±3	95±6	95±5	93±5	93±5
EN AC-AlSi9Cu3(Fe) UNE-EN 1706-2011	min 80	–	–	–	–

As explained before, hardness values are at the same level for both degassing treatments, which indicates that grain size is in a similar level for both materials. Grain refining may take place when the ultrasonic treatment is conducted in a melt with a reduced superheat and shortly before the solidification takes place [14, 15]. In the present work, the metal was treated at a temperature of more than 100°C over the liquidus of the alloy and between the ultrasonic treatment and the alloy solidification at least several minutes passed and a transfer movement occurred and these processing conditions may prevent grain refining [19].

4. CONCLUSIONS

From the results obtained, the following conclusions can be inferred from the present study:

- The ultrasonic technology at a prototype level studied in this article shows a better degassing efficiency, lowering the hydrogen content in a large industrial melt volume of 500 kg of AlSi9Cu3(Fe) by 28% to 36% when compared to the work of a porous lance, a commercially available degassing technology.
- The better degassing efficiency of the US treatment is mitigated by the HPDC process, obtaining castings with a similar porosity level to lance degassing.
- The obtained hardness values are well above the minimum values established in the standard for the alloy and are similar for the different treatment conditions analysed, suggesting that the present experimental set-up does not promote a grain refining effect on the final component.

Acknowledgements

The authors would like to acknowledge the financial support provided by the European Union's Seventh Framework Program managed by REA – Research Executive Agency (FP7/2007-2013) under Grant Agreement number 286344 (www.doshormat.eu). The authors gratefully acknowledge all of the help provided by the members of the consortium.

REFERENCES

[1] Campbell J. (2003). *Castings*, 2nd Ed. Oxford: Butterworth--Heinemann.
[2] Eskin G. & Eskin D. (2014). *Ultrasonic Treatment of Light Alloy Melts*, 2nd Ed. Boca Raton: CRC Press.
[3] Eskin D., Alba-Baena N., Pabel T. & da Silva M. (2015). Ultrasonic degassing of aluminium alloys: basic studies and practical implementation. *Materials Science and Technolgy*, 31(1), 79–84. Doi: https://doi.org/10.1179/1743284714Y.0000000587.
[4] Esmarch W., Rommel T. & Benther K. (1940). *Werkstoff-Sonderheft*. Berlin: W.V. Siemens Werke, 78–87.
[5] Bradfield G. (1950). Summarized Proceedings of Symposium on Applications of Ultrasonics. *Proceedings of the Physical Society B*, 305–321. Doi: https://doi.org/10.1088/0370-1301/63/5/301.
[6] Eskin G. (1965). Ul'trazvukovaya obrabotka rasplavlennogo alyuminiya [*Ultrasonic Treatment of Molten Aluminum*]. Moskva: Metallurgija. [Эскин Г. (1965). *Ультразвуковая обработка расплавленного алюминия*. Москва: Металлургия].
[7] Xu H., Meek T.T. & Han Q. (2008). Effect of ultrasonic vibration on degassing of aluminium alloy. *Materials Science and Engineering A*, 473(1–2), 96–104. Doi: https://doi.org/10.1016/j.msea.2007.04.040.
[8] Puga H., Barbosa J., Tuan N.Q. & Silva G. (2004). Effect of ultrasonic degassing on performance of Al-based components. *Transactions of Nonferrous Metals Society of China*, 24 (11), 3459–3464. Doi: https://doi.org/10.1016/S1003-6326(14)63489-0.
[9] Galarraga H., Garcia de Cortazar M., Arregi E., Iparraguirre J.A. & Oncala J.L. (2018). Improved ultrasonic degassing of AlSi10Mg alloy and its performance evaluation with reducer pressure test (RPT) method. *The 73rd World Foundry Congress: September 23–27. Krakow*. World Foundry Association Ltd., 337–338.
[10] da Silva M., Rebolledo L., Pabel T., Petkov T., Planta X., Tort J. & Eskin D. (2015). Evaluation of effect of ultrasonic degassing on components produced by low pressure die casting. *International Journal of Cast Metals Research*, 28 (4), 193–200. Doi: https://doi.org/10.1179/1743133614Y.0000000141.
[11] Ignaszak Z. & Hajkowski J. (2015). Contribution to the Identification of Porosity Type in AlSiCu High-Pressure-Die-Castings by Experimental and Virtual Way. *Archives of Foundry Engineering*, 15(1), 143–151.
[12] Niklas A., Orden S., Bakedano A., da Silva M., Nogués E. & Fernández-Calvo A.I. (2016). Effect of solution heat treatment on gas porosity and mechanical properties in a die cast step test part manufactured with a new AlSi10MnMg(Fe) secondary alloy. *Materials Science and Engineering A*, 667(14), 376–382. Doi: https://doi.org/10.1016/j.msea.2016.05.024.
[13] Mondolfo L.F. (1976). *Aluminum Alloys. Structure & Properties*. London: Butterworth & Co., 759–805.
[14] Powell M., Manchiraju K. & Han Q. (2016). Ultrasonic grain refining of continuous cast aluminium: microstructure and properties. *TMS Conference Light Metals: February 14–18. Nashvile*, 737–740. Doi: https://doi.org/10.1007/978-3-319--48251-4_124.
[15] Haghayeghi R., Ezzatneshan E. & Bahai H. (2015). Grain refinement of AA5754 aluminium alloy by ultrasonic cavitation: experimental study and numerical simulation. *Metals and Materials International,* 21, 109–117. Doi: https://doi.org/10.1007/s12540-014-6015-5.
[16] Ghassemali E., Riestra M., Bogdanoff T., Bharath S. Kumar & Seifaddine S. (2017). Hall–Petch equation in a hypoetutectic Al-Si cast alloy: grain size vs. secondary dendrite arm spacing. *Procedia Engineering*, 207, 19–24. Doi: https://doi.org/10.1016/j.proeng.2017.10.731.
[17] Basavakumar K.G., Mukunda P.G., Chakraborty M. (2008). Influence of grain refinement and modification on microstructure and mechanical properties of Al-7Si and Al-7Si-2.5Cu cast alloys. *Materials Characterization*, 283–289. Doi: https://doi.org/10.1016/j.matchar.2007.01.011.
[18] Tiryakioglu M., Campbell J., Staley J. (2000). Hardness-Strength Relationships in Cast Al-Si-Mg Alloys. *Materials Science Forum*, 331–337, 295–300. Doi: https://doi.org/10.4028/www.scientific.net/MSF.331-337.295.
[19] Piatkowski J., Przeliorz R., Gontarczyk A. (2016). The study of phase transformations of AlSi9Cu3 alloy by DSC method, *Archives of Foundry Engineering*, 16 (4), 109–112. Doi: https://doi.org/10.1515/afe-2016-0093.